

High energy X-ray diffraction study of novel cathode materials for rechargeable magnesium-ion batteries during magnesium insertion/extraction

Ichiro Inoue¹ and Yuta Tashiro²

Department of Advanced Materials Science, Graduate School of Frontier Sciences,

The University of Tokyo, Kashiwanoha, Kashiwa, Chiba, Japan

¹inoue@x-ray.k.u-tokyo.ac.jp ²yuta.tashiro@gmail.com

1. About the authors

Ichiro Inoue: As a Ph.D. student of Prof. Amemiya group, he has involved research on developments and applications of advanced X-ray techniques using synchrotron sources and X-ray free-electron lasers. After he earned M.D. from Univ. Tokyo, he joined beamline scientist group of SPring-8 Ångstrom Compact free-electron LAser (SACLA) in Hyogo, where he has developed femtosecond X-ray-X-ray pump-probe experiments, photon-beam diagnostic systems, and methodologies to generate attosecond hard X-ray pulses. In the study shown below, he performed X-ray diffraction experiments at SPring-8, and analyzed the experimental data.

Yuta Tashiro: A member of Takagi lab in department of advanced materials science. I shifted the theme of research development of thermoelectric materials to that of ion-battery materials. I moved to Sendai 1 year ago. I like Sendai because of delicious marine products!

2. Backgrounds and purpose

Rechargeable ion batteries, especially Lithium ion-batteries (LIBs), have been one of the most common energy storages for various kinds of electric devices around us, such as laptop computers, mobile phones, and digital cameras. Although the usage of has been expanding, further improvements in safety and capacity are crucially required.

One of the potential candidates for realizing such improvements is Magnesium ion-batteries (MIBs). Compared with Li-ion, Mg-ion has high thermodynamic stability, and thus MIBs are expected to assure much reliable safety. Furthermore, divalency of Mg-ion should contribute to higher capacities. Realization of high performance-MIBs is, however, quite difficult. The major obstacle is development of cathode materials. Although many researches had performed so far, very limited number of cathode materials for MIBs has been reported. This is probably because strong interaction between Mg-ion and ions in the host lattice prevents rechargeability of batteries [1]. To solve this problem, Tashiro think that the materials that have very close energy levels between *d* orbitals of transition metals and

Final Report on MERIT Self-directed Joint Research

those of p orbitals of anions, *i.e.*, strong d - p hybridization, would weak traps of mobile ions, because charge delocalization is enhanced.

Based on this idea, Tashiro searched candidates for cathode materials in MIBs, and found that TiSe_2 and VSe_2 realize large capacity (over 100 mAh/g) with high rechargeability. Although these materials show brilliant macroscopic properties, we have not understood detailed mechanism during Mg-ion insertion/extraction processes. To clarify the microscopic mechanism, such as 1: which crystallographic sites are occupied by Mg-ion and 2: how much degree of Mg-ion are inserted/extracted for each site, we applied X-ray powder diffraction measurement to TiSe_2 and VSe_2 during Mg-ion insertion/extraction processes.

3. Experimental section

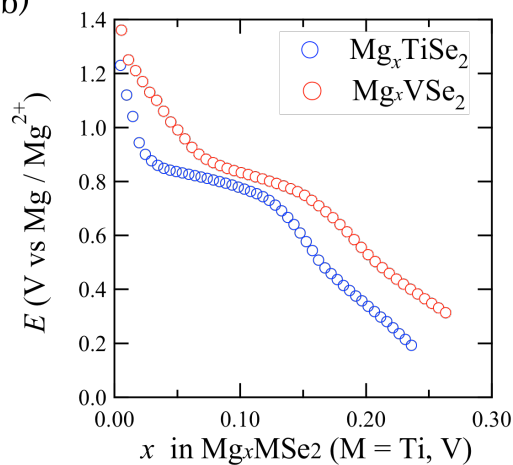
3-1. Sample preparation

Powder of TiSe_2 and VSe_2 purchased from Kojundo chemical laboratory were used for sample preparations. These reagents were mixed with carbon black (CB) and polytetrafluoroethylene (PTFE), and the weight ratio was TiSe_2 (or VSe_2): CB : PTFE = 81 : 9 : 10. Cu mesh was used as current collector. These mixtures were pasted on current collectors. We used this as cathodes. Anode was Mg ribbon and electrolyte was $\text{Mg}(\text{AlCl}_2\text{EtBu})_2/\text{THF}$ solution. These were assembled into coin cell (Fig.1(a)). Keeping current density 50 mAh/g, Mg ions were inserted/extracted several times. The mole number of Mg ions were estimated from discharging curve (Fig.1(b)). We prepared 8 samples: powder samples of Mg_xTiSe_2 ($x=0, 0.13, 0.13, 0.24$), Mg_xVSe_2 ($x=0, 0.082, 0.26$) and sample pasted on Cu mesh Mg_xVSe_2 ($x=0.24$). (There were two kinds of $\text{Ti}_{0.13}\text{Se}_2$ samples.)

(a)



(b)



Final Report on MERIT Self-directed Join Research

Figure 1: (a) Coin cell used for these experiments, (b) Discharging curve of TiSe_2 and VSe_2

3-2. Powder diffraction method

We performed high-energy powder diffraction experiments at room temperature at SPring-8 BL44B2[1] using Debye-Scherrer camera (camera radius: 286.48 nm) equipped at the beamline [2]. Powder samples packed in Ar atmosphere were fixed to Gonio head as shown in Fig.2. 26.5 keV-X-ray beams were collimated to be 3mm (horizontal) x 0.5 mm (vertical). The exposure time for each sample was set to be 120 seconds. To reduce the influences occurred by selective orientations of the samples, samples were swung 10° during X-ray diffractions.

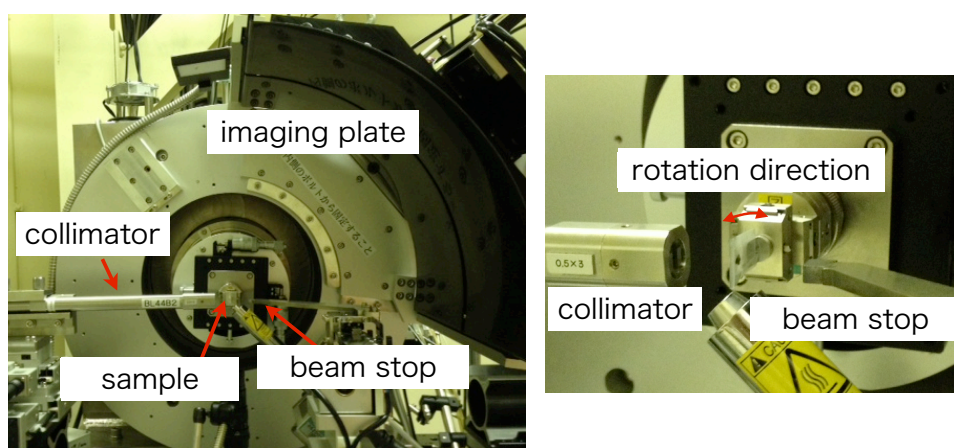


Figure 2: Debye-Scherrer camera and experimental geometry.

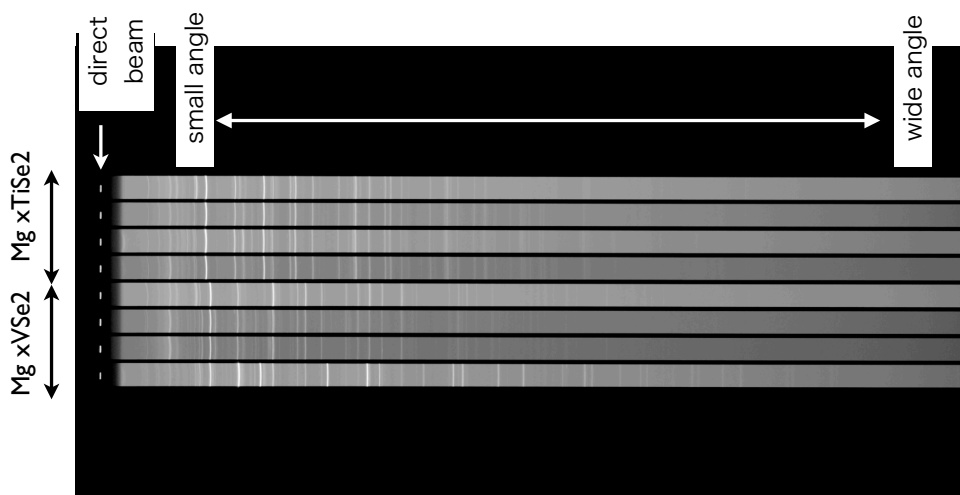


Figure 3: Diffraction line profiles measured with an imaging plate. From top, diffraction line profiles correspond to TiSe_2 , $\text{Mg}_{0.13}\text{TiSe}_2$, $\text{Mg}_{0.13}\text{TiSe}_2$, $\text{Mg}_{0.24}\text{TiSe}_2$, VSe_2 , $\text{Mg}_{0.082}\text{VSe}_2$, $\text{Mg}_{0.26}\text{VSe}_2$, and $\text{Mg}_{0.10}\text{VSe}_2$ pasted on Cu mesh, respectively.

4. Results and discussion

Figure 3 shows diffraction line profiles measured with an imaging plate (IP). The IP covered the diffraction angles ranging from 2° to 75° . If we compared the diffraction peaks of $\text{Mg}_{0.082}\text{VSe}_2$ and $\text{Mg}_{0.10}\text{VSe}_2$ pasted on Cu mesh, we can see additional peaks for $\text{Mg}_{0.10}\text{VSe}_2$, which can be considered to be diffraction signals from Cu mesh. Since peak intensities from Cu mesh were larger than those of $\text{Mg}_{0.082}\text{VSe}_2$ pasted on Cu mesh, we performed the following analysis only for powder samples.

4-1. Changes in lattice constants during Mg insertion process

For the first step, we assumed that contribution from diffractions of Mg ions is negligibly small. Under this assumption we determined lattice constants and atomic positions of Mg_xTiSe_2 and Mg_xVSe_2 by applying Rietveld analysis [5]. Typical examples of experimental data and fitting result are shown in Fig.4. It can be clearly seen that the fitting curve well describes the experimental data in wide-angle intensity profile ($2\theta > 30^\circ$), which indicates that main phases in samples were TiSe_2 or VSe_2 .

The determined lattice constants and the unit cell volume are shown in Table 1. It was found that changes in lattice constants caused by insertion of Mg^{2+} were less than 0.05 \AA . According to Shannon's table [6], ionic radius of 6-coordinated Mg^{2+} is 86 pm and effective volume of Mg^{2+} is estimated to be around 3 \AA^3 . The magnitude of effective volume is too small to elucidate insertion of Mg^{2+} into TiSe_2 and VSe_2 . Thus, our experimental results

claims that Mg-ions were absorbed by other impurities, rather than inserted into TiSe_2 or VSe_2 . To verify this assumption, we tried to characterize impurities absorbing Mg-ion.

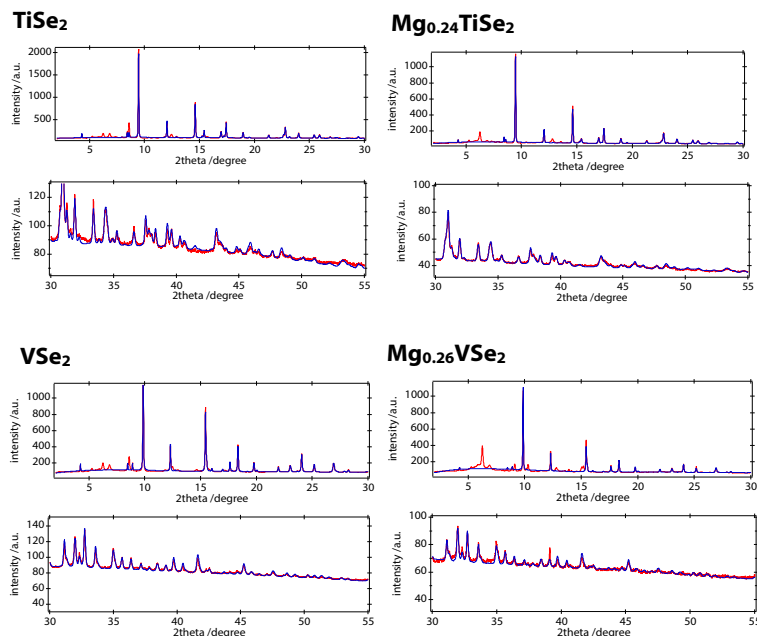


Fig.4 Intensity profiles measured by the experiment (red line) and their fitting results by Rietveld analysis without considering contribution from Mn^{2+} (blue line).

	a /Å	b /Å	c /Å	α (fix)	β (fix)	γ (fix)	Volume/Å ³
TiSe₂	3.54334 ±0.00017	3.54334 ±0.00017	6.01679 ±0.00017	90	90	120	65.42
Mg_{0.13}TiSe₂	3.54639 ±0.00017	3.54639 ±0.00018	6.03300 ±0.00088	90	90	120	65.71
Mg_{0.13}TiSe₂	3.54866 ±0.00027	3.54866 ±0.00027	6.05261 ±0.00084	90	90	120	66.01
Mg_{0.24}TiSe₂	3.53933 ±0.00023	3.53933 ±0.00023	6.02217 ±0.00092	90	90	120	65.33
VSe₂	3.35337 ±0.00016	3.35337 ±0.00016	6.10122 ±0.00060	90	90	120	59.42
Mg_{0.082}VSe₂	3.35741 ±0.00039	3.35741 ±0.00039	6.10648 ±0.00115	90	90	120	59.61
Mg_{0.26}VSe₂	3.35628 ±0.00033	3.35628 ±0.00033	6.10636 ±0.00129	90	90	120	59.57

Table 1: Unit cell parameters determined by Rietveld analysis.

4-2. Characterization of impurities

If you see closely diffraction peaks of Mg_xTiSe_2 and Mg_xVSe_2 at small-angle region, you can find several peaks at the same scattering angle for both materials. According to crystallographic database, we deduced that these peaks corresponds diffraction signals from Selenium and presumed that Selenium is an impurity contributing Mg-ion absorption and discharge. To investigate this presumption, we performed Rietveld analysis for the mixture of Selenium and Mg_xTiSe_2 samples.

Figure 5 shows the results of this Rietveld analysis of Mg_xTiSe_2 . Compared the experimental data with the fitting results, intensity ratio of Selenium and Mg_xTiSe_2 became smaller as the amount of absorbed Mg^{2+} increased. Similar tendency was observed for Mg_xVSe_2 . This result indicates that Selenium change into other chemical compounds during Mg-ion absorption. The ratio of Selenium to $TiSe_2$ was determined to be 0.26 by the above fitting, which is almost same the maximum number of absorbed Mg ion (around $x=0.25$). This finding indicates that Selenium or Selenium compounds play important roles during absorption of Mg ions.

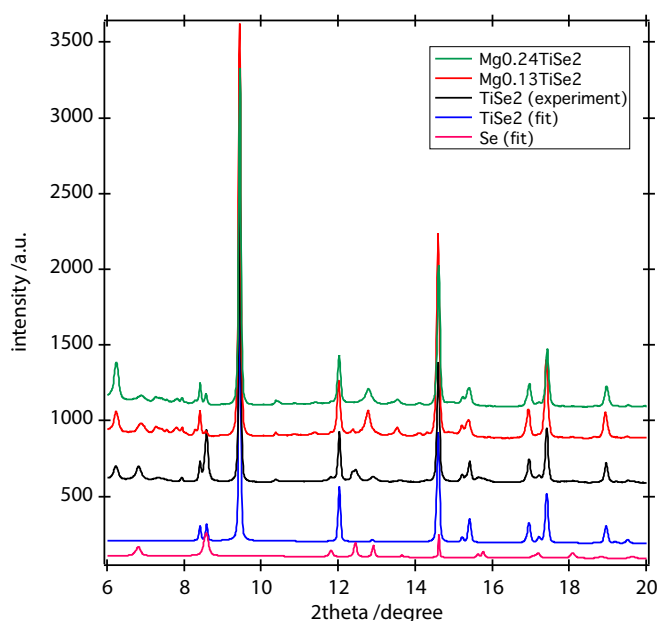


Fig.5 Diffraction intensity profile of Mg_xTiSe_2 samples ($x=0, 0.13, 0.24$) and its fitting results by Rietveld analysis assuming impurity of Selenium.

5. Conclusion and future plans

At first, we aim to reveal the microscopic mechanism of Mg-ion insertion/extraction processes in TiSe_2 and VSe_2 . Precise analysis with high energy-X-ray beams, however, indicated that Mg ions are not inserted into the layers of TiSe_2 or VSe_2 , but absorbed by Selenium compound. To identify the Selenium compound contributing Mg-ion absorption, we synthesized several candidates, and finally we found that Cu_2Se would play the main role for Mg-ion absorption in the measured samples. Since it was experimentally found that this compound shows high performance for cathode materials in Mg ion battery (electric capacity: 120 mAh/g), we are trying to optimize the performance of this compound by nano-crystal synthesis.

6. Acknowledgements

We are grateful for our supervisors: Prof. Y. Amemiya, Prof. H. Takagi, Prof. K. Tanigushi, Prof. T. Arima, and Prof. K. Kimura, for permitting this collaborative research. We also acknowledge thank to Prof. E. Shishibori of Univ. Tsukuba for his technical support for experiments at SPring-8. Last but not least, we thank the MERIT program for giving us a chance to collaboration research.

Reference

- [1] <http://www.spring8.or.jp/wkg/BL44B2/instrument/lang-en/INS-0000000381/view>
- [2] E. Nishibori *et al.*, *Nucl. Instrum. Methods Phys. Res. A* **467-468**, 1045 (2001).
- [3] J. Miyahara *et al.*, *Nucl. Instrum. Methods Phys. Res. A* **246**, 572 (1986).
- [4] Y. Amemiya and J. Miyahara, *Nature* **336**, 89 (1988).
- [5] H. M. Rietveld, *J. Appl. Cryst.* **2**, 65 (1969).
- [6] R. D. Shanon, *Acta. Cryst. A* **32**, 751 (1976).